



UvA-DARE (Digital Academic Repository)

Scalable Synthesis of Robust MOF for Challenging Ethylene Purification and Propylene Recovery with Record Productivity

Wang, G.-D.; Li, Y.-Z.; Krishna, R.; Zhang, W.-Y.; Hou, L.; Wang, Y.-Y.; Zhu, Z.

DOI

[10.1002/ange.202319978](https://doi.org/10.1002/ange.202319978)

[10.1002/anie.202319978](https://doi.org/10.1002/anie.202319978)

Publication date

2024

Document Version

Final published version

Published in

Angewandte Chemie

License

Article 25fa Dutch Copyright Act (<https://www.openaccess.nl/en/policies/open-access-in-dutch-copyright-law-taverne-amendment>)

[Link to publication](#)

Citation for published version (APA):

Wang, G.-D., Li, Y.-Z., Krishna, R., Zhang, W.-Y., Hou, L., Wang, Y.-Y., & Zhu, Z. (2024). Scalable Synthesis of Robust MOF for Challenging Ethylene Purification and Propylene Recovery with Record Productivity. *Angewandte Chemie*, 136(15), Article e202319978. <https://doi.org/10.1002/ange.202319978>, <https://doi.org/10.1002/anie.202319978>

General rights

It is not permitted to download or to forward/distribute the text or part of it without the consent of the author(s) and/or copyright holder(s), other than for strictly personal, individual use, unless the work is under an open content license (like Creative Commons).

Disclaimer/Complaints regulations

If you believe that digital publication of certain material infringes any of your rights or (privacy) interests, please let the Library know, stating your reasons. In case of a legitimate complaint, the Library will make the material inaccessible and/or remove it from the website. Please Ask the Library: <https://uba.uva.nl/en/contact>, or a letter to: Library of the University of Amsterdam, Secretariat, Singel 425, 1012 WP Amsterdam, The Netherlands. You will be contacted as soon as possible.



Scalable Synthesis of Robust MOF for Challenging Ethylene Purification and Propylene Recovery with Record Productivity

Gang-Ding Wang[†], Yong-Zhi Li[†], Rajamani Krishna, Wen-Yan Zhang, Lei Hou,^{*} Yao-Yu Wang, and Zhonghua Zhu

Abstract: Ethylene (C₂H₄) purification and propylene (C₃H₆) recovery are highly relevant in polymer synthesis, yet developing physisorbents for these industrial separation faces the challenges of merging easy scalability, economic feasibility, high moisture stability with great separation efficiency. Herein, we reported a robust and scalable MOF (MAC-4) for simultaneous recovery of C₃H₆ and C₂H₄. Through creating nonpolar pores decorated by accessible N/O sites, MAC-4 displays top-tier uptakes and selectivities for C₂H₆ and C₃H₆ over C₂H₄ at ambient conditions. Molecular modelling combined with infrared spectroscopy revealed that C₂H₆ and C₃H₆ molecules were trapped in the framework with stronger contacts relative to C₂H₄. Breakthrough experiments demonstrated exceptional separation performance for binary C₂H₆/C₂H₄ and C₃H₆/C₂H₄ as well as ternary C₃H₆/C₂H₆/C₂H₄ mixtures, simultaneously affording record productivities of 27.4 and 36.2 L kg⁻¹ for high-purity C₂H₄ (≥ 99.9 %) and C₃H₆ (≥ 99.5 %). MAC-4 was facilely prepared at deckgram-scale under reflux condition within 3 hours, making it as a smart MOF to address challenging gas separations.

Introduction

Global demand for propylene (C₃H₆) and ethylene (C₂H₄) which are important chemical feedstocks in downstream manufacture industry is increasing,^[1,2] with a total global production of beyond 300 million tons in 2023.^[3,4] C₃H₆ and C₂H₄ are traditionally produced from the crude oil cracking or dehydrogenation process. Considerable attention has been recently paid to producing C₃H₆ and C₂H₄ from natural gas, coal, biomass, and methanol-to-olefins (MTO) reaction.^[5] In these processes, C₂H₄ products inevitably comprise small of ethane (C₂H₆) impurities at 6–10 %, while the products of MTO reaction mainly contain C₃H₆ of 20.9 wt % and C₂H₄ of 51.1 wt %.^[6,7] Therefore, the follow-up separation by cryogenic distillation cycling operated under high pressure and low temperature conditions is essential to derive polymer-grade olefins since their highly close physicochemical properties.^[8–10] Replacing distillation technology by adsorption separation using porous adsorbents would bring tremendous global benefits due to high efficiency, energy saving, and environmental friendliness.^[11–13]

Metal–organic frameworks (MOFs) as an emerging type of customizable adsorbents with abundant functionality and structural modularity offer a promising platform for addressing the task-specific requirements of various applications,^[14–18] especially in gas separation and purification.^[19–24] For C₂H₆/C₂H₄ separation, the utilization of C₂H₆-selective MOFs is more desirable owing to pure C₂H₄ products can be directly obtained through one-step separation process, avoiding additional desorption step that is indispensably for C₂H₄-selective MOFs and greatly reducing energy consumption.^[25–28] However, C₂H₆-selective MOFs were not well developed, in particularly they usually suffer from “trade-off” effect with either low selectivity because of the difficulty in discriminating C₂H₄ and C₂H₆ or low adsorption capacity owing to small available voids.^[29,30] This trouble makes it be a constant challenge in designing C₂H₆-selective MOFs.

The latest research demonstrated that the creation of open metal sites (OMSs) in MOFs is effective for C₃H₆/C₂H₄ separation, wherein the OMSs bind the C=C π units in C₃H₆ and C₂H₄ by M⋯π interactions with different strengths.^[7,31] However, this strategy is not judicious for designing C₂H₆-selective MOFs since C₂H₄ are more easily adsorbed by OMSs. As high contents of C₂H₄ and C₃H₆ in MTO products, the collection of high-purity C₂H₄ and C₃H₆ through separating C₃H₆/C₂H₄ mixtures is important for the

[*] Dr. G.-D. Wang,[†] Dr. Y.-Z. Li,[†] Prof. W.-Y. Zhang, Prof. L. Hou, Prof. Y.-Y. Wang
Key Laboratory of Synthetic and Natural Functional Molecule of the Ministry of Education
College of Chemistry & Materials Science, Northwest University
Xi'an, 710069, P. R. China.
E-mail: lhou2009@nwu.edu.cn

Prof. R. Krishna
Van't Hoff Institute for Molecular Sciences University of Amsterdam
Science Park 904, 1098 XH Amsterdam, The Netherlands

Dr. Y.-Z. Li[†]
School of Materials and Physics, China University of Mining and Technology
Xuzhou 221116, P. R. China.

Prof. Z. Zhu
School of Chemical Engineering, The University of Queensland
Brisbane 4072, Australia

[†] These authors contributed equally to this work.

downstream application of olefins. However, at present the simultaneous recovery of C_3H_6 and C_2H_4 by MOFs was only reported in one example.^[32] So it is of great industrial and academic interest to develop the MOFs for separating both C_2H_6/C_2H_4 and C_3H_6/C_2H_4 mixtures to afford pure C_2H_4 and C_3H_6 , respectively. Besides, the real challenge remaining for C_2H_4 purification technology through MOFs could lie in the scale-up synthesis and affordable cost of the materials upon maintaining the separation performance. Currently, most of the reported C_3H_6 - or C_2H_6 -selective MOFs suffer from high production cost, poor stability or synthesis scalability, severely hindering their practical utilization. To date, the efficient C_3H_6 - and C_2H_6 -selective MOFs that satisfied all the above requirements have not been reported. Thus, it is extremely essential to develop MOFs that merge the factor regarding to excellent separation performance, while remains a daunting challenge.

A handful of C_2H_6 -selective MOFs containing nonpolar pore surfaces (e.g., aliphatic or aromatic moieties) have been recently evidenced to be certainly beneficial for preferentially adsorbing C_2H_6 over C_2H_4 based on the slightly higher polarizability of C_2H_6 ($44.7 \times 10^{25} \text{ cm}^{-3}$) over C_2H_4 ($42.52 \times 10^{25} \text{ cm}^{-3}$).^[25,33] In addition, there were also some MOFs that mainly relied on well-designed available interacting sites (e.g. N/O atoms), leading to more hydrogen bonds with C_2H_6 and C_3H_6 than C_2H_4 .^[34,35] With the above considerations in mind, we supposed that design nonpolar pore environments with N/O active sites in MOFs could display the potential for both C_2H_6/C_2H_4 and C_3H_6/C_2H_4 separation. Herein, we developed a highly stable MOF, MAC-4 [$Zn_5(\text{dmtrz})_3(\text{ipa})_3(\text{OH})$], fabricated by Zhou et al.^[36] This material is composed of inexpensive and easily available ligands of isophthalic acid ($H_2\text{ipa}$) and 3,5-dimethyl-1,2,4-triazole (Hdmtrz) ligands. In particular, it contains nonpolar pores with rich O/N sites and inorganic secondary building units (SBUs) without undesired OMSs, these two structure features would be very favourable for the target function of C_2H_6 - and C_3H_6 selectivity over C_2H_4 in MOFs. MAC-4 displayed not only high uptakes and selectivities for C_2H_6 and C_3H_6 over C_2H_4 but also efficient one-step purification of C_2H_4 from C_2H_6/C_2H_4 and C_3H_6/C_2H_4 mixtures with high C_2H_4 productivity of 21.6 L kg^{-1} and 349.3 L kg^{-1} , respectively. MAC-4 also provided a record high C_3H_6 ($\geq 99.5\%$) recovery capacity of 70.1 L kg^{-1} in single C_3H_6/C_2H_4 separation process, as well as one-step acquisition of C_2H_4 ($\geq 99.9\%$) and C_3H_6 ($\geq 99.5\%$) from $C_3H_6/C_2H_6/C_2H_4$ mixtures. GCMC calculations unveiled that multiple N/O active sites in nonpolar pores provided stronger interactions with both C_3H_6 and C_2H_6 over C_2H_4 .

Results and Discussion

MAC-4 with an orthorhombic $Pnma$ space group was built on two types of cluster-based SBUs: paddle-wheel [$Zn_2(\text{COO})_4$] and triangle [$Zn_3(\text{OH})(\text{dmtrz})_3$]. The same SBUs are connected by ipa^{2-} linkers or Zn–N coordination bonds to produce one-dimensional chains along the b and a axes, respectively (Figure 1a and S1). The linkage between two

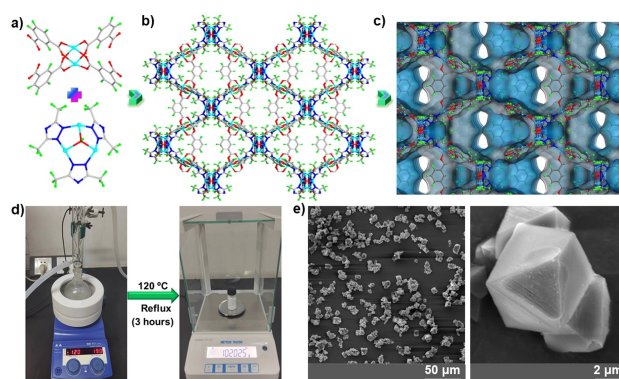


Figure 1. a) [$Zn_2(\text{COO})_4$] and [$Zn_3(\text{OH})(\text{dmtrz})_3$] SBUs, b) and c) 3D structure of MAC-4 (H, green; Zn, turquoise; C, gray; O, red; N, blue); d) photographs of the deckgram-scale synthesis of MAC-4; e) SEM images of MAC-4 microcrystalline with octahedral bulk.

types of SBUs through coordination interactions generates a 3D porous network. Remarkably, the framework with the void of $\sim 45.5\%$ contains 1D zig-zag open channels (size $\sim 5.9\text{--}8.0 \text{ \AA}$) that were decorated by the methyl groups of dmtrz, phenyl rings of ipa^{2-} ligands as well as rich N and O sites (Figure 1b and 1c).

In the pursuit of convenient synthesis methods, it was important to find that MAC-4 could be rapidly and easily synthesized through refluxing the reactants in DMF within 3 hours with a high yield (78%). The phase purity and crystallinity of the MAC-4 microcrystalline were verified by scanning electron microscope (SEM) and powder X-ray diffraction (PXRD) tests (Figure 1d, 1e and S2). Thermogravimetric analysis (TGA) displayed a continuous weight loss; however, the CH_2Cl_2 -exchanged samples showed a wide thermostable plateau up to 350°C following an initial weight loss before 140°C (Figure S3).

Nitrogen (N_2) adsorption isotherms at 77 K showed type-I curves for the scaled-up and single-crystal MAC-4 samples with the saturated loadings of 338 and $343 \text{ cm}^3 \text{ g}^{-1}$, respectively, indicating the close Brunauer–Emmett–Teller (BET) surface areas of 1180 and $1218 \text{ m}^2 \text{ g}^{-1}$ (Figure S4). The pore size distribution of $6.4\text{--}10.8 \text{ \AA}$ agrees with the calculated results from crystal structure. The accessible porous wall of MAC-4 is mainly modified by phenyl rings and methyl groups in ligands, giving rise to a hydrophobic environment, as confirmed by the water vapour adsorption showing a type-V isotherm at 298 K (Figure S5). The structure of MAC-4 after both activation and water adsorption was intact, as demonstrated by PXRD (Figure S2).

The suitable pore size and nonpolar pore environment of MAC-4 inspired us to examine its C_2H_4 purification performance. First, the sorption isotherms of different shape of MAC-4 samples prepared from solvothermal (crystals) and reflux (microcrystalline) reactions were measured at 273 and 298 K (Figure S6–S8). Both samples displayed very close sorption isotherms for C_2H_6 , C_2H_4 , and C_3H_6 , demonstrated no difference in adsorption performance between the samples. MAC-4 showed typical type-I sorption iso-

therms for C_2H_6 , C_2H_4 , and C_3H_6 with the uptakes of 107/124, 83/108, and 127/140 $cm^3 g^{-1}$ at 100 kPa and 298/273 K, respectively (Figure 2a and S9). The C_2H_6 uptake in MAC-4 is remarkably higher than most top-performing C_2H_6 -selective materials, such as MUF-15,^[37] Azole-Th-1,^[38] NKCOF-21,^[39] TJT-100,^[30] $Fe_2(O_2)dobdc$,^[40] MAF-49^[41] and so on, and is slightly lower than benchmark MOFs CPM-233^[42] and ZJU-120a^[43] (Figure S10). MAC-4 also shows exceptional loadings of 56, 42, and 108 $cm^3 g^{-1}$ for C_2H_6 , C_2H_4 , and C_3H_6 at a high temperature of 353 K (Figure 2b). Meanwhile, the adsorption curves of MAC-4 exhibit higher uptakes and steeper slopes for C_3H_6 and C_2H_6 than C_2H_4 , indicating selective adsorption of C_3H_6 and C_2H_6 over C_2H_4 . These findings are in accord with the calculated values of adsorption enthalpy (Q_{st}) at zero coverage with the order of C_3H_6 ($25.3 kJ mol^{-1}$) > C_2H_6 ($22.7 kJ mol^{-1}$) > C_2H_4 ($17.1 kJ mol^{-1}$) (Figure 2c). It was noted that the Q_{st} data showed inflection points for three gases, in particular for C_3H_6 and C_2H_6 , from zero-coverage to 1.5, 1.0, and 1.0 $mmol g^{-1}$ loadings for C_3H_6 , C_2H_6 , and C_2H_4 gases, respectively, which corresponded to the amounts of gas molecules in one pore were about 1.7, 1, and 1 molecules. The inflection points for Q_{st} data could be because of the reorientation of gas molecules in pores under increased pressure. Meanwhile, due to relatively high loadings, the interactions between the C_3H_6 molecules in pores could also be responsible for the obviously increased Q_{st} of C_3H_6 .^[37] Notably, the Q_{st} values of three gases are below 32 $kJ mol^{-1}$ owing to the nonpolar pores of MAC-4, implying a facile regeneration treatment with low energy consumption. In fact, the fully reproducible C_3H_6 , C_2H_6 , and C_2H_4 adsorption curves can be recycled with the simple activation treatment (353 K for 10 minutes) prior to each cycle (Figure S11–13).

Given that the real-industrial application environment, the material must possess long-term and high humidity stability. The stability of MAC-4 toward air environments and humidity was evaluated and monitored by gas adsorptions and PXRD measurements. As divulged in Figure 2d

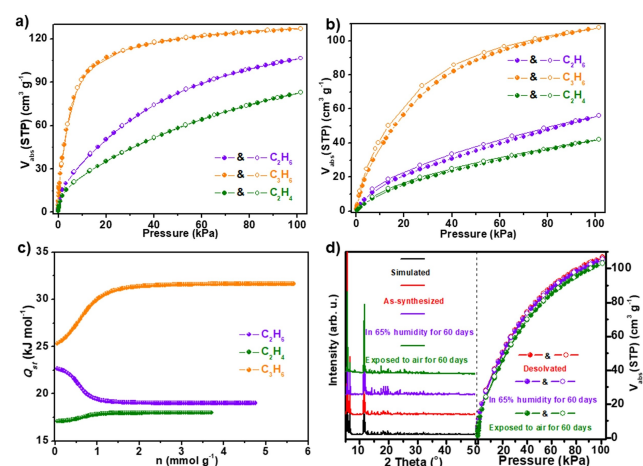


Figure 2. a) Sorption isotherms of MAC-4 at 298 K; b) sorption isotherms of MAC-4 at 353 K; c) Q_{st} curves; d) PXRD patterns (left) and C_2H_6 adsorption isotherms (right) of MAC-4 samples.

(left), after exposing to 65 % humidity and air environment for 60 days, MAC-4 remains intact without crystallinity loss and phase transformation, as verified by PXRD. Moreover, the adsorption isotherms for C_2H_6 at 298 K for above samples are very close to that of the initial samples, confirming and guaranteeing the great stability of MAC-4 for practical utilization (Figure 2d right).

As for higher uptakes and larger adsorption enthalpies toward C_3H_6 and C_2H_6 than C_2H_4 , the separation selectivities of MAC-4 for C_2H_6/C_2H_4 and C_3H_6/C_2H_4 mixtures were evaluated by employing ideal adsorbed solution theory (Figure S14–S16). For C_2H_6/C_2H_4 mixtures, MAC-4 displays high initial selectivities of 2.0/2.3/3.8, 2.0/2.4/4.1, and 2.0/2.4/4.2 for 1/1, 1/9, and 1/15 mixtures at 353/298/273 K, respectively, and which are still high of 1.7/1.9/2.2 at 100 kPa (Figure 3a, S17, and S19). These selectivities are higher than or comparable to many well-developed C_2H_6 -selective adsorbents, e.g. SNUU-40,^[44] CPOC-301,^[45] NKCOF-22,^[39] and TJT-100.^[30] For C_3H_6/C_2H_4 mixtures, the selectivity values were calculated to be 8.6/9.5/16.2, 8.4/10.6/19.2, and 8.1/10.9/20.6 for 1/1, 2/5, and 1/9 C_3H_6/C_2H_4 mixtures at 353/298/273 K, respectively (Figure 3b, S18, and S19), which are only lower than $Zn_2(ob)_2(dmipym)$,^[34] but significantly larger than most of materials, such as Mn-dpzip,^[31] NEM-7-Cu,^[46] and Zn-BPZ-SA^[35] (Figure S20). At the same time, the separation potential (ΔQ) that was reported by Krishna and integrated the advantages of selectivity and capacity was utilized to evaluate the separation performance, which reflects the maximum C_2H_4 productivity.^[47,48] For equimolar C_2H_6/C_2H_4 mixtures, ΔQ were calculated to be 0.5, 1.3, and 1.9 $mmol g^{-1}$ at 353, 298, and 273 K, respectively (Figure S21), outdoing the most advanced C_2H_6 -selective adsorbents, such as MUF-15,^[37] NKCOF-23,^[39] CPOC-301,^[45] and Tb-MOF-76(NH_2),^[49] under the same conditions (Figure 3c). The corresponding ΔQ values for equimolar C_3H_6/C_2H_4 mixtures are 3.2, 4.4, and 5.3 $mmol g^{-1}$ at 353, 298, and 273 K, respectively (Figure S22), superior to some well-

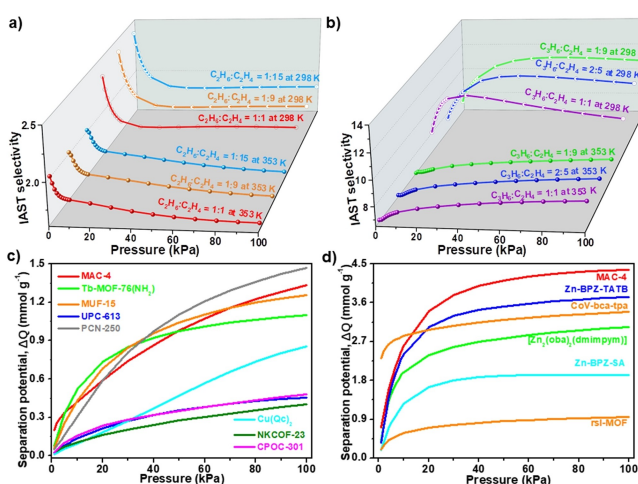


Figure 3. a) and b) IAST selectivities of MAC-4 for C_2H_6/C_2H_4 and C_3H_6/C_2H_4 mixtures; comparisons of separation potential for C_2H_6/C_2H_4 (c) and C_3H_6/C_2H_4 (d) mixtures in MAC-4 and other adsorbents at 298 K.

developed MOFs, e.g. $[\text{Zn}_2(\text{oba})_2(\text{dmimpym})]$,^[34] Zn-BPZ-SA ,^[35] CoV-bca-tca ,^[50] and Zn-BPZ-TATB ^[32] (Figure 3d).

To gain precise insight into the preferential adsorption sites of C_3H_6 , C_2H_4 , and C_2H_6 in MAC-4, molecular modelling was performed based on Grand Canonical Monte Carlo (GCMC) simulations. All three gas molecules were preferentially located at the cavities formed around two $[\text{Zn}_2(\text{COO})_4]$ SBUs and two triazolate-trinuclear $[\text{Zn}_3(\text{OH})(\text{dmtrz})_3]$ SBUs. One C_2H_4 interacts with three carboxylate O atoms and two triazolate N atoms through quintuple $\text{C-H}\cdots\text{O/N}$ hydrogen bonds ($\text{H}\cdots\text{O/N}=2.88\text{--}3.19\text{ \AA}$) (Figure 4a). In comparison, the interactions between the framework and $\text{C}_3\text{H}_6/\text{C}_2\text{H}_6$ molecules are more and stronger, in which C_2H_6 is bound to four N atoms from $[\text{Zn}_3(\text{OH})(\text{dmtrz})_3]$ SBUs and three O atoms through seven $\text{C-H}\cdots\text{O/N}$ hydrogen bonds ($\text{H}\cdots\text{O}=2.85\text{--}3.19\text{ \AA}$) (Figure 4b). For C_3H_6 , it not only is involved in nine $\text{C-H}\cdots\text{O/N}$ hydrogen bonds ($\text{H}\cdots\text{O}=2.79\text{--}3.26\text{ \AA}$), but also forms one $\text{C-H}\cdots\pi$ interaction via the alkenyl π clouds of C_3H_6 (Figure 4c). Therefore, the MOF possesses a greater affinity for C_2H_6 and C_3H_6 relative to C_2H_4 . Meanwhile, the calculated binding energies also showed larger values for C_3H_6 (37.3 kJ mol^{-1}) and C_2H_6 (35.7 kJ mol^{-1}) compared to C_2H_4 (31.5 kJ mol^{-1}).

The interactions of C_2H_4 , C_3H_6 , and C_2H_6 with MAC-4 were deliberated at 100 kPa and 298 K by further simulations. As divulged in Figure S23–S26, two C_2H_4 , three C_2H_6 , and four C_3H_6 molecules mainly interacted with the pore walls. Two C_2H_4 via the $-\text{CH}$ units form multiple $\text{C-H}\cdots\text{O/N}$ contacts with triazolate N atoms and carboxylate O atoms (Figure S23). Three C_2H_6 molecules are located in different coordination fragments interacting with N/O atoms through $\text{C-H}\cdots\text{O/N}$ hydrogen bonds ($\text{H}\cdots\text{O/N}=2.65\text{--}3.29\text{ \AA}$) (Figure S24). C_3H_6 molecules are involved in more contacts not only with the accessible N/O atoms but also with the π centers and methyl groups from linkers. Specifically, C_3H_6 -I

and C_3H_6 -II exist in similar locations around two $[\text{Zn}_2(\text{COO})_4]$ SBUs through $\text{C-H}\cdots\text{O}/\pi$ contacts ($\text{H}\cdots\text{O}=2.69\text{--}3.17\text{ \AA}$, $\text{H}\cdots\pi=2.86\text{--}3.32\text{ \AA}$) with carboxylate O atoms and phenyl π centers as well as $\text{C-H}\cdots\pi$ interactions between two C_3H_6 molecules (Figure S25). C_3H_6 -III and C_3H_6 -IV are resided in the region of $[\text{Zn}_3(\text{OH})(\text{dmtrz})_3]$ fragments through forming multiple $\text{C-H}\cdots\text{C/O/N}$ hydrogen bonds and $\text{C-H}\cdots\pi$ interactions with the ligands (Figure S26). Meanwhile, these multiple contacts for C_3H_6 and C_2H_6 molecules can also be confirmed by the higher values of interaction energy (E) distributions for C_3H_6 ($\bar{E}=56.9\text{ kJ mol}^{-1}$) and C_2H_6 ($\bar{E}=41.8\text{ kJ mol}^{-1}$) compared to C_2H_4 ($\bar{E}=34.7\text{ kJ mol}^{-1}$) (Figure S27). The simulation results are in accordance with the experimental findings and well explain the high selectivities for both C_3H_6 and C_2H_6 over C_2H_4 .

Breakthrough experiments were performed at 273, 298, and 353 K for $\text{C}_2\text{H}_6/\text{C}_2\text{H}_4$ (v/v, 5/5, 1/9, and 1/15) mixtures under Ar as the carrier gas (vol %, 90 %, 90 % and 84 %, a total flow of 7 mL min^{-1}), in which the mixtures were passed through the packed column. As shown in Figure 5a–5c, three mixtures can be completely separated by MAC-4, in which C_2H_4 was first outflowed from the column to directly get pure C_2H_4 ($\geq 99.9\%$), while C_2H_6 was adsorbed in the bed for a certain period of times. During this process, 1 kg MAC-4 can retrieve high-purity C_2H_4 ($\geq 99.9\%$) about 5.4, 14.9, and 21.6 L from 5/5, 1/9, and 1/15 $\text{C}_2\text{H}_6/\text{C}_2\text{H}_4$ mixtures at 298 K, respectively. The breakthrough experiments for the higher concentrations of $\text{C}_2\text{H}_6/\text{C}_2\text{H}_4$ mixtures (10/10, 20/20, 30/30, v/v) were also tested at 273 and 298 K (Figure S28–S30), and it also displayed the complete separation of the mixtures. Moreover, the cycling experiments showed no loss of separation ability in MAC-4, illustrating outstanding reusability (Figure S31).

The difficult scalability and high cost of MOF adsorbents has long been a troubled issue for their application. In general, the cost of MOFs primarily depends on ligands. Although some MOFs display benchmark performance for $\text{C}_2\text{H}_6/\text{C}_2\text{H}_4$ separation, they suffer from long-time (48–72 h)

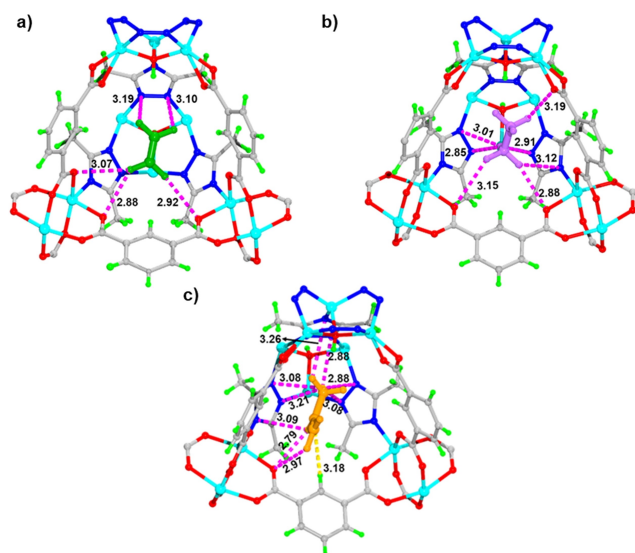


Figure 4. Preferential adsorption sites for a) C_2H_4 , b) C_2H_6 , and c) C_3H_6 (H, green; Zn, turquoise; C, gray; O, red; N, blue).

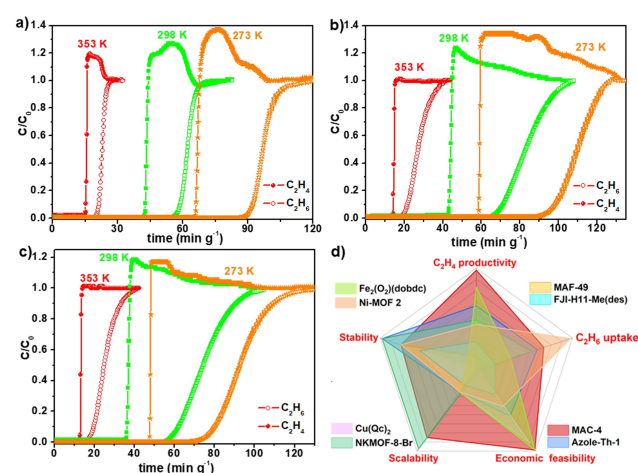


Figure 5. a–c) Breakthrough curves for $\text{C}_2\text{H}_6/\text{C}_2\text{H}_4$ mixtures at 273, 298, and 353 K: a) 1/1, b) 1/9, c) 1/15; d) comprehensive comparisons for MAC-4 and other porous materials.

heating synthesis conditions and the use of expensive ligands, such as 2-bromoimidazole-4,5-dicarbonitrile of NKMOF-8-Br (142 \$g⁻¹), 2,3,5,6-tetramethylterephthalic acid of Ni(TMBDC)(DABCO)_{0.5} (309 \$g⁻¹), 4-(1H-tetrazol-5-yl) benzoic acid of Azole-Th-1 (62 \$g⁻¹), and 4,4',4'',4'''-(ethene-1,1,2,2-tetrayl) tetrabenzoic acid of NUM-7a (309 \$g⁻¹).^[28] In contrast, MAC-4 could be facilely deckgram-scalably prepared through stirring within 3 hours from commercially available cheap reagents with a cost of about 1 \$g⁻¹ (Table S2). Taken together, MAC-4 not only displays promising C₂H₆/C₂H₄ separation performance, but also satisfies several crucial criteria for an industrial adsorbent including high stability, scalability, and economic feasibility, rendering it to be one of benchmark material to address challenges on C₂H₄ purification in industrial application (Figure 5d).

The breakthrough experiments for various ratios of C₃H₆/C₂H₄ (v/v: 20/20, 10/25, and 4/36) mixtures with Ar as carrier gas (vol %: 60 %, 65 %, and 60 %) were also conducted to appraise the separation for MTO products. As presented in Figure 6a, 6b, S32, S33 and S34, highly efficient separation for the mixtures can be achieved by MAC-4, whereby C₂H₄ eluted through the column to directly yield an outflow of pure C₂H₄ (≥99.9 %), but C₃H₆ was adsorbed for a long time. About 125.1, 210.6, and 349.3 L of pure C₂H₄ (≥99.9 %) could be trapped from 20/20, 10/25, and 4/36 C₃H₆/C₂H₄ mixtures, respectively, for 1 kg MAC-4 at 298 K in one cycle, surpassing all-known C₃H₆-selective adsorbents, such as iso-MOF-4,^[7] [Zn₂(oba)₂(dmimpym)],^[34] Fe₂Mn-L,^[51] and Zn-BPZ-SA.^[35] As C₃H₆ is another target gas that needs to be purified from MTO products, the desorption experiments were then performed to determine C₃H₆ purity and productivity. Upon reaching equilibrium concentration, the adsorption-saturated MAC-4 was purged by Ar gas (7 mlmin⁻¹) at 323 K. As shown in Figure 6a and 6b, the

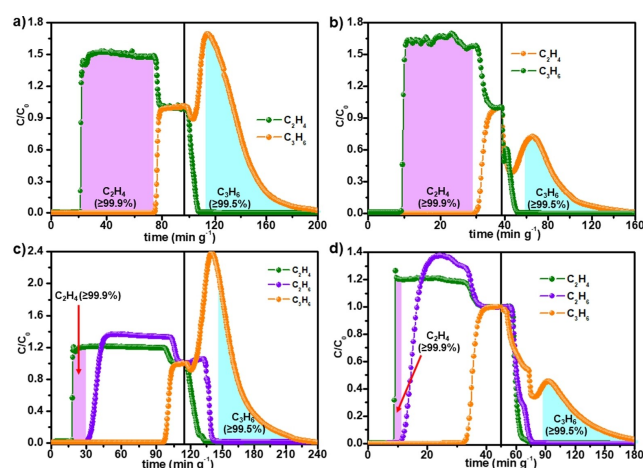


Figure 6. a) Breakthrough curves for C₃H₆/C₂H₄ (v/v, 20/20) mixtures at 298 K; b) breakthrough curves for C₃H₆/C₂H₄ (v/v, 20/20) mixtures at 353 K; c) breakthrough curves for the C₂H₆/C₃H₆/C₂H₄ mixture (v/v/v, 2/10/25) mixtures at 298 K; d) breakthrough curves for the C₂H₆/C₃H₆/C₂H₄ mixture (v/v/v, 2/10/25) mixtures at 353 K, after adsorption-saturated, the desorption curves obtained under Ar (7 mLmin⁻¹) sweeping at 323 K.

samples can be easily regenerated, in which the adsorbed C₂H₄ was desorbed more quickly than C₃H₆ owing to weaker binding affinity of MAC-4 for C₂H₄. It was estimated that 36.8 and 70.1 Lkg⁻¹ of C₃H₆ (≥99.5 %) could be produced from C₃H₆/C₂H₄ (v/v, 20/20) mixtures at 353 and 298 K, respectively. To our best knowledge, these productivities of C₂H₄ and C₃H₆ obtained through MAC-4 separation are highest in reported materials.

Although MAC-4 achieved efficient C₂H₄ purification and C₃H₆ recovery from binary C₃H₆/C₂H₄ mixtures, there are tremendous current impediments and challenges in the recovery of high-valuable C₃H₆ from MTO products due to that typically contains few other light hydrocarbons. Thus, the separation experiments for ternary C₂H₆/C₃H₆/C₂H₄ (v/v/v, 2/10/25 and 5/5/5) mixtures at 353 and 298 K were tested. For the 2/10/25 C₂H₆/C₃H₆/C₂H₄ mixtures at 298 K, it showed that at the column outlet highly pure C₂H₄ (≥99.9 %) flowed out firstly, with a 27.4 Lkg⁻¹ productivity, following by C₂H₆ after 29.5 min g⁻¹, while C₃H₆ was retained in the column as long as 95.8 min g⁻¹. After adsorption saturation, the desorption steps were carried out by purging with Ar gas (7 mlmin⁻¹) at 323 K to evaluate the feasibility of C₃H₆ recovery. As depicted in Figure 6c, C₂H₄ and C₂H₆ were rapidly desorbed from MAC-4 within 30 min g⁻¹, then the high-purity C₃H₆ (≥99.5 %) with a 36.2 Lkg⁻¹ productivity was recovered. Therefore, the pure C₃H₆ and C₂H₄ with record-high productivities can be respectively obtained from C₂H₆/C₃H₆/C₂H₄ mixtures in one single adsorption/desorption operation. Furthermore, when the ratios of mixtures were adjusted to 5/5/5 or the temperature was rose to 353 K, MAC-4 still exhibited prominent separation ability (Figure 6d, S35, and S36). These results evidently demonstrated that MAC-4 might deliver pure both C₂H₄ and C₃H₆ from imitative MTO products. Furthermore, multiple breakthrough tests demonstrated no decrease of separation performance at least five continuous cycles (Figure S37), confirming good regeneration of MAC-4. Overall, MAC-4 combines the advances of benchmark C₂H₆/C₂H₄ and C₃H₆/C₂H₄ separation performance, ultrahigh moisture stability as well as scale-up synthesis, making it an outstanding adsorbent for C₂H₄ purification and C₃H₆ recovery application.

Next, transient breakthrough simulations were carried out for the exact same set of operating conditions as in the above mentioned experiments, using the methodology described in earlier publications.^[52–55] In these simulations, intra-crystalline diffusion influences are ignored. There is good match between the experiments and simulations in every case (Figure S38–S45). Having established the accuracy of the transient breakthrough simulations, transient breakthrough simulations for the C₂H₆/C₂H₄ (50/50, v/v), C₃H₆/C₂H₄ (50/50, v/v), and C₃H₆/C₂H₆/C₂H₄ (33.33/33.33/33.33, v/v/v) mixtures without inert gas were performed at 298 and 353 K and 100 kPa to evaluate the practical applications for C₂H₄ purification of MAC-4. The results in Figure 7 clearly demonstrate that MAC-4 is capable of separating three mixtures, whereby C₂H₄ elutes first in all cases and subsequently reached a plateau to produce polymer-grade C₂H₄ before C₂H₆ and C₃H₆ breakthrough

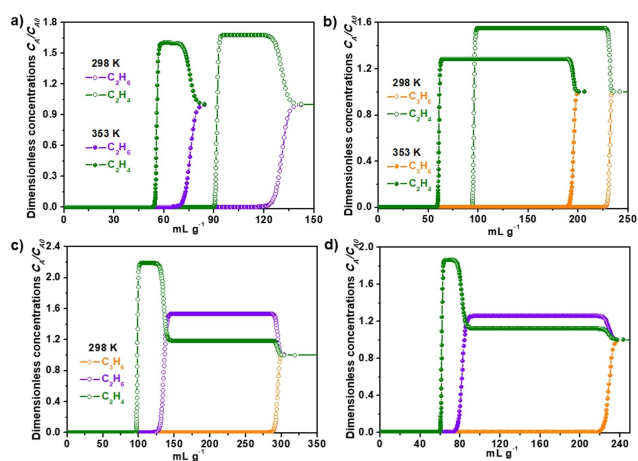


Figure 7. a) Simulated breakthrough curves of MAC-4 for C_2H_6/C_2H_4 (50/50) at 298 and 353 K; b) C_3H_6/C_2H_4 (50/50) at 298 and 353 K; c) $C_3H_6/C_2H_6/C_2H_4$ (33.33/33.33/33.33) at 298 K; d) $C_3H_6/C_2H_6/C_2H_4$ (33.33/33.33/33.33) at 353 K, the x-axis is not min g^{-1} but mL g^{-1} .

occurred. Based on the simulated breakthrough curves, MAC-4 can directly produce 8.2, 64.5, and 5.9 L kg^{-1} C_2H_4 (purity > 99.9%) from C_2H_6/C_2H_4 , C_3H_6/C_2H_4 , and $C_3H_6/C_2H_6/C_2H_4$ at 353 K, respectively. The corresponding C_2H_4 productivity values at 298 K are 23.6, 94.3, and 18.9 L kg^{-1} , respectively. The C_2H_4 productivity for C_2H_6/C_2H_4 (50/50, v/v) are obviously higher than most C_2H_6 -selective adsorbents, such as $\text{Fe}_2(\text{O}_2)\text{dobdc}$ ^[40] and JNU-2,^[56] Ni-MOF 2,^[25] HOF-76a,^[57] MAF-49,^[41] NKMOF-14-PD,^[58] and HOF-NBDA-(DMA)^[59] (Figure S46).

In addition, the separation performance of MAC-4 was explored at a crucial low pressure by the simulated density distributions of equimolar binary C_2H_6/C_2H_4 and C_3H_6/C_2H_4 mixtures as well as ternary $C_3H_6/C_2H_6/C_2H_4$ mixtures. As predicted in Figure 8a and 8b, for the inlet of binary C_2H_6/C_2H_4 or C_3H_6/C_2H_4 mixtures under 20 kPa, the density

distributions of mixture gases are concentrated at the corners of ipa^{2-} ligands and methyl group near the coordinated units in the framework. Although single-component adsorption site simulation results show that the coordinated units interact with C_2H_4 , but for the mixtures the adsorption sites are more occupied by C_3H_6 or C_2H_6 molecules compared to C_2H_4 . These findings coincided with the preferentially competitive adsorption for C_3H_6 and C_2H_6 molecules in the framework. Meanwhile, for $C_3H_6/C_2H_6/C_2H_4$ mixtures at 15 kPa, the density distributions of three gas molecules also deferred to the order of $C_3H_6 > C_2H_6 \gg C_2H_4$ (Figure 8c), revealing the preferential adsorption and significant selectivity for C_3H_6 and C_2H_6 over C_2H_4 , which further verified the excellent separation performance of MAC-4.

To further probe the gas binding sites, infrared (IR) spectroscopies of MAC-4 with the loading of C_3H_6 , C_2H_6 , and C_2H_4 were measured. Figure 8d shows an apparent and new stretching bands at 3050–2850 and 1646 cm^{-1} that belong to C_3H_6 in C_3H_6 -loaded MAC-4.^[60] Besides, tiny changes at 1558 and 1537 cm^{-1} were observed, suggesting that C_3H_6 molecule formed the interactions with triazole rings (Figure S47).^[61] Similarly, when C_2H_6 was loaded into MAC-4, characteristic peaks (2980 cm^{-1}) assigned to fundamental $\nu(\text{CH}_3)$ stretches of C_2H_6 molecule appeared (Figure 8e).^[26,58] Meanwhile, the tiny changes at 1553 and 1538 cm^{-1} were also observed, indicating that C_2H_6 had multiple interactions with triazole rings (Figure S48). In contrast, no distinct peak change for C_2H_4 -loaded MAC-4 was observed, which could be attributed to the weak interactions between C_2H_4 and the framework (Figure 8f). These IR spectroscopies qualitatively and partly supported the simulated results.

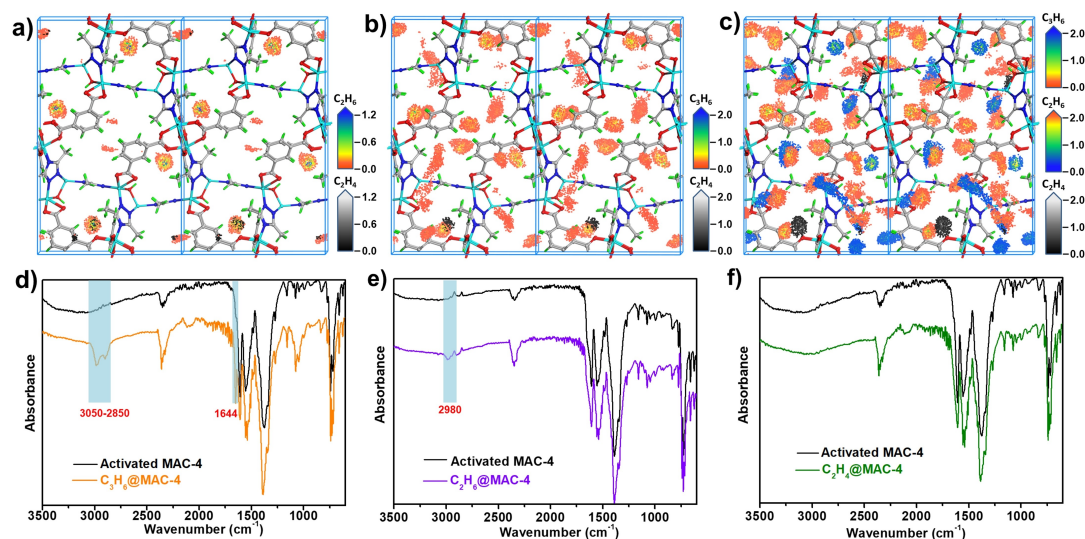


Figure 8. Simulated density distributions in MAC-4 for C_2H_6/C_2H_4 (a), C_2H_6/C_2H_4 (b), and $C_3H_6/C_2H_6/C_2H_4$ (c) mixtures; d-f) IR spectra of activated MAC-4, $C_3H_6@MAC-4$, $C_2H_6@MAC-4$ and $C_2H_4@MAC-4$.

Conclusions

In conclusion, we developed a deckgram-scale synthetic route of cheap and robust MOF MAC-4 with the goal of C₂H₄ purification from C₂H₆ and C₃H₆ mixtures. The non-polar pore surfaces with accessible O/N active sites endow the MOF with preferential adsorption for C₃H₆ and C₂H₆ over C₂H₄, leading to simultaneously high C₂H₆ and C₃H₆ uptakes and significant C₃H₆/C₂H₄ and C₂H₆/C₂H₄ selectivity. MAC-4 not only directly produces high-purity C₂H₄ (≥ 99.9%) from C₂H₆/C₂H₄ and C₃H₆/C₂H₄ mixtures, but also provides a high C₃H₆ (≥ 99.5%) recovery capacity through one adsorption-desorption procedure, which are highest in known materials. In addition, MAC-4 also realized one-step acquisition of C₂H₄ (99.9%) and C₃H₆ (99.5%) with the record productivities of 27.4 and 36.2 L kg⁻¹ from C₃H₆/C₂H₆/C₂H₄ ternary mixtures. The comprehensive advantages on moisture stability, scalability, economic feasibility, separation performance, and reusability laid a solid foundation for MAC-4 to be applied in C₂H₄ purification and C₃H₆ recovery from the corresponding mixtures. This presentation would march an important step toward challenging C₂H₆/C₂H₄ and C₃H₆/C₂H₄ separation in applications and would facilitate the development of MOF-based adsorbents for new separation target as well.

Acknowledgements

This work is supported by National Natural Science Foundation of China (22371226 and 22371225) and Natural Science Basic Research Program of Shaanxi (2024JC-JCQN-18).

Conflict of Interest

The authors declare no conflict of interest.

Data Availability Statement

The data that support the findings of this study are available in the supplementary material of this article.

Keywords: metal–organic framework · scalable synthesis · gas adsorption and separation · ethylene purification · propylene recovery

- [1] Y. Wang, T. Li, L. Li, R.-B. Lin, X. Jia, Z. Chang, H.-M. Wen, X.-M. Chen, J. Li, *Adv. Mater.* **2023**, *35*, 2207955.
- [2] P. Zhang, L. Yang, X. Liu, J. Wang, X. Suo, L. Chen, X. Cui, H. Xing, *Nat. Commun.* **2022**, *13*, 4928.
- [3] P. Hu, J. Hu, H. Liu, H. Wang, J. Zhou, R. Krishna, H. Ji, *ACS Cent. Sci.* **2022**, *8*, 1159–1168.
- [4] Z. Di, C. Liu, J. Pang, S. Zou, Z. Ji, F. Hu, C. Chen, D. Yuan, M. Hong, M. Wu, *Angew. Chem. Int. Ed.* **2022**, *61*, e202210343.
- [5] H. M. T. Galvis, J. H. Bitter, C. B. Khare, M. Ruitenbeek, A. I. Dugulan, K. P. De Jong, *Science* **2012**, *335*, 835–838.

- [6] G.-D. Wang, Y.-Z. Li, W.-J. Shi, L. Hou, Y.-Y. Wang, Z. Zhu, *Angew. Chem. Int. Ed.* **2022**, *61*, e202205427.
- [7] W. Fan, X. Wang, X. Zhang, X. Liu, Y. Wang, Z. Kang, F. Dai, B. Xu, R. Wang, D. Sun, *ACS Cent. Sci.* **2019**, *5*, 1261–1268.
- [8] D. S. Sholl, R. P. Lively, *Nature* **2016**, *532*, 435–437.
- [9] S. Jiang, J. Li, M. Feng, R. Chen, L. Guo, Q. Xu, L. Chen, F. Shen, Z. Zhang, Y. Yang, Q. Ren, Q. Yang, Z. Bao, *J. Mater. Chem. A* **2022**, *10*, 24127–24136.
- [10] L. Yang, S. Qian, X. Wang, X. Cui, B. Chen, H. Xing, *Chem. Soc. Rev.* **2020**, *49*, 5359–5406.
- [11] Y. Yang, L. Li, R.-B. Lin, Y. Ye, Z. Yao, L. Yang, F. Xiang, S. Chen, Z. Zhang, S. Xiang, B. Chen, *Nat. Chem.* **2021**, *13*, 933–939.
- [12] K.-J. Chen, D. G. Madden, S. Mukherjee, T. Pham, K. A. Forrest, A. Kumar, B. Space, J. Kong, Q.-Y. Zhang, M. J. Zaworotko, *Science* **2019**, *366*, 241–246.
- [13] D.-D. Zhou, J.-P. Zhang, *Acc. Chem. Res.* **2022**, *55*, 2966–2977.
- [14] G.-D. Wang, Y.-Z. Li, W.-J. Shi, B. Zhang, L. Hou, Y.-Y. Wang, *Sens. Actuators B* **2021**, *331*, 129377.
- [15] X.-R. Tian, Z.-Y. Jiang, S.-L. Hou, H.-S. Hu, J. Li, B. Zhao, *Angew. Chem. Int. Ed.* **2023**, *62*, e202301764.
- [16] Q. Yin, Z. Song, S. Yang, G.-D. Wang, Y. Sui, J. Qi, D. Zhao, L. Hou, Y.-Z. Li, *Chem. Sci.* **2023**, *14*, 5643–5649.
- [17] G. Hu, Q. Liu, Y. Zhou, W. Yan, Y. Sun, S. Peng, C. Zhao, X. Zhou, H. Deng, *J. Am. Chem. Soc.* **2023**, *145*, 13181–13194.
- [18] W. Yang, Q. Liu, J. Yang, J. Xian, Y. Li, G. Li, C.-Y. Su, *CCS Chem.* **2022**, *4*, 2276–2285.
- [19] S.-Q. Yang, R. Krishna, H. Chen, L. Li, L. Zhou, Y.-F. An, F.-Y. Zhang, Q. Zhang, Y.-H. Zhang, W. Li, T.-L. Hu, X.-H. Bu, *J. Am. Chem. Soc.* **2023**, *145*, 13901–13911.
- [20] C. Yu, Z. Guo, L. Yang, J. Cui, S. Chen, Y. Bo, X. Suo, Q. Gong, S. Zhang, X. Cui, S. He, H. Xing, *Angew. Chem. Int. Ed.* **2023**, *62*, e202218027.
- [21] D. Liu, J. Pei, X. Zhang, X.-W. Gu, H.-M. Wen, B. Chen, G. Qian, B. Li, *Angew. Chem. Int. Ed.* **2023**, *62*, e202218590.
- [22] Z. Zhang, Z. Deng, H. A. Evans, D. Mullangi, C. Kang, S. B. Peh, Y. Wang, C. M. Brown, J. Wang, P. Canepa, A. K. Cheetham, D. Zhao, *J. Am. Chem. Soc.* **2023**, *145*, 11643–11649.
- [23] Y. Jiang, Y. Hu, B. Luan, L. Wang, R. Krishna, H. Ni, X. Hu, Y. Zhang, *Nat. Commun.* **2023**, *14*, 401.
- [24] H. Zeng, M. Xie, T. Wang, R.-J. Wei, X.-J. Xie, Y. Zhao, W. Lu, D. Li, *Nature* **2021**, *595*, 542–548.
- [25] Y. Ye, Y. Xie, Y. Shi, L. Gong, J. Phipps, A. M. Al-Enizi, A. Nafady, B. Chen, S. Ma, *Angew. Chem. Int. Ed.* **2023**, *62*, e202302564.
- [26] S. Geng, E. Lin, X. Li, W. Liu, T. Wang, Z. Wang, D. Sensharma, S. Darwish, Y. H. Andaloussi, T. Pham, P. Cheng, M. J. Zaworotko, Y. Chen, Z. Zhang, *J. Am. Chem. Soc.* **2021**, *143*, 8654–8660.
- [27] S.-Q. Yang, T.-L. Hu, *Coord. Chem. Rev.* **2022**, *468*, 214628.
- [28] D. Lv, P. Zhou, J. Xu, S. Tu, F. Xu, J. Yan, H. Xi, W. Yuan, Q. Fu, X. Chen, Q. Xia, *Chem. Eng. J.* **2022**, *431*, 133208.
- [29] Q. Ding, Z. Zhang, Y. Liu, K. Chai, R. Krishna, S. Zhang, *Angew. Chem. Int. Ed.* **2022**, *61*, e202208134.
- [30] H.-G. Hao, Y.-F. Zhao, D.-M. Chen, J.-M. Yu, K. Tan, S. Ma, Y. Chabal, Z.-M. Zhang, J.-M. Dou, Z.-H. Xiao, G. Day, H.-C. Zhou, T.-B. Lu, *Angew. Chem. Int. Ed.* **2018**, *57*, 16067–16071.
- [31] L. Zhang, L.-N. Ma, G.-D. Wang, L. Hou, Z. Zhu, Y.-Y. Wang, *J. Mater. Chem. A* **2023**, *11*, 2343–2348.
- [32] G.-D. Wang, Y.-Z. Li, W.-J. Shi, L. Hou, Y.-Y. Wang, Z. Zhu, *Angew. Chem. Int. Ed.* **2023**, *62*, e202311654.
- [33] M. Kang, D. W. Kang, J. H. Choe, H. Kim, D. W. Kim, H. Park, C. S. Hong, *Chem. Mater.* **2021**, *33*, 6193–6199.
- [34] Y.-Z. Li, G.-D. Wang, R. Krishna, Q. Yin, D. Zhao, J. Qi, Y. Sui, L. Hou, *Chem. Eng. J.* **2023**, *466*, 143056.

- [35] G.-D. Wang, R. Krishna, Y.-Z. Li, Y.-Y. Ma, L. Hou, Y.-Y. Wang, Z. Zhu, *ACS Materials Lett.* **2023**, *5*, 1091–1099.
- [36] Y. Ling, F. Yang, M. Deng, Z. Chen, X. Liu, L. Weng, Y. Zhou, *Dalton Trans.* **2012**, *41*, 4007–4011.
- [37] O. T. Qazvini, R. Babarao, Z.-L. Shi, Y.-B. Zhang, S. G. Telfer, *J. Am. Chem. Soc.* **2019**, *141*, 5014–5020.
- [38] Z. Xu, X. Xiong, J. Xiong, R. Krishna, L. Li, Y. Fan, F. Luo, B. Chen, *Nat. Commun.* **2020**, *11*, 3163.
- [39] F. Jin, E. Lin, T. Wang, S. Geng, T. Wang, W. Liu, F. Xiong, Z. Wang, Y. Chen, P. Cheng, Z. Zhang, *J. Am. Chem. Soc.* **2022**, *144*, 5643–5652.
- [40] L. Li, R.-B. Lin, R. Krishna, H. Li, S. Xiang, H. Wu, J. Li, W. Zhou, B. Chen, *Science* **2018**, *362*, 443–446.
- [41] P.-Q. Liao, W.-X. Zhang, J.-P. Zhang, X.-M. Chen, *Nat. Commun.* **2015**, *6*, 8697.
- [42] H. Yang, Y. Wang, R. Krishna, X. Jia, Y. Wang, A. N. Hong, C. Dang, H. E. Castillo, X. Bu, P. Feng, *J. Am. Chem. Soc.* **2020**, *142*, 2222–2227.
- [43] J. Pei, J.-X. Wang, K. Shao, Y. Yang, Y. Cui, H. Wu, W. Zhou, B. Li, G. Qian, *J. Mater. Chem. A* **2020**, *8*, 3613–3620.
- [44] Y.-P. Li, Y.-N. Zhao, S.-N. Li, D.-Q. Yuan, Y.-C. Jiang, X. Bu, M.-C. Hu, Q.-G. Zhai, *Adv. Sci.* **2021**, *8*, 2003141.
- [45] K. Su, W. Wang, S. Du, C. Ji, D. Yuan, *Nat. Commun.* **2021**, *12*, 3703.
- [46] X. Liu, C. Hao, J. Li, Y. Wang, Y. Hou, X. Li, L. Zhao, H. Zhu, W. Guo, *Inorg. Chem. Front.* **2018**, *5*, 2898–2905.
- [47] R. Krishna, *RSC Adv.* **2017**, *7*, 35724–35737.
- [48] R. Krishna, *ACS Omega* **2020**, *5*, 16987–17004.
- [49] G.-D. Wang, R. Krishna, Y.-Z. Li, W.-J. Shi, L. Hou, Y.-Y. Wang, Z. Zhu, *Angew. Chem. Int. Ed.* **2022**, *61*, e202213015.
- [50] Y. Xiao, A. N. Hong, Y. Chen, H. Yang, Y. Wang, X. Bu, P. Feng, *Small* **2023**, *19*, 2205119.
- [51] X.-M. Liu, L.-H. Xie, Y. Wu, *Materials* **2023**, *16*, 154.
- [52] R. Krishna, *Microporous Mesoporous Mater.* **2014**, *185*, 30–50.
- [53] R. Krishna, *RSC Adv.* **2015**, *5*, 52269–52295.
- [54] R. Krishna, *Sep. Purif. Technol.* **2018**, *194*, 281–300.
- [55] R. Krishna, *Precision Chemistry* **2023**, *1*, 83–93.
- [56] H. Zeng, X.-J. Xie, M. Xie, Y.-L. Huang, D. Luo, T. Wang, Y. Zhao, W. Lu, D. Li, *J. Am. Chem. Soc.* **2019**, *141*, 20390–20396.
- [57] X. Zhang, L. Li, J.-X. Wang, H.-M. Wen, R. Krishna, H. Wu, W. Zhou, Z.-N. Chen, B. Li, G. Qian, B. Chen, *J. Am. Chem. Soc.* **2020**, *142*, 633–640.
- [58] W. Liu, S. Geng, N. Li, S. Wang, S. Jia, F. Jin, T. Wang, K. A. Forrest, T. Pham, P. Cheng, Y. Chen, J.-G. Ma, Z. Zhang, *Angew. Chem. Int. Ed.* **2023**, *62*, e202217662.
- [59] Y. Zhou, C. Chen, R. Krishna, Z. Ji, D. Yuan, M. Wu, *Angew. Chem. Int. Ed.* **2023**, *62*, e202305041.
- [60] Y. Xie, Y. Shi, E. M. C. Morales, A. E. Karch, B. Wang, H. Arman, K. Tan, B. Chen, *J. Am. Chem. Soc.* **2023**, *145*, 2386–2394.
- [61] H.-M. Wen, C. Yu, M. Liu, C. Lin, B. Zhao, H. Wu, W. Zhou, B. Chen, J. Hu, *Angew. Chem. Int. Ed.* **2023**, *62*, e202309108.

Manuscript received: December 24, 2023

Accepted manuscript online: February 18, 2024

Version of record online: March 1, 2024